Received: 15 February 2024 | Revised: 15 May 2024 | Accepted: 17 May 2024

DOI: 10.1002/jcc.27442

RESEARCH ARTICLE

Journal of COMPUTATIONAL CHEMISTRY WILEY

Carbamic acid and its dimer: A computational study

Cristina Puzzarini | Silvia Alessandrini

Department of Chemistry "Giacomo Ciamician", University of Bologna, Bologna, Italy

Correspondence
Cristina Puzzarini, Department of Chemistry "Giacomo Ciamician", University of Bologna, Via F. Selmi 2, Bologna, 40126, Italy.
Email: cristina.puzzarini@unibo.it

Funding information
MUR, Grant/Award Number: 202082CE3T; University of Bologna (RFO funds)

Abstract

A recent work by Marks et al. on the formation of carbamic acid in NH_3-CO_2 interstellar ices pointed out its stability in the gas phase and the concomitant production of its dimer. Prompted by these results and the lack of information on these species, we have performed an accurate structural, energetic and spectroscopic investigation of carbamic acid and its dimer. For the former, the structural and spectroscopic characterization employed composite schemes based on coupled cluster (CC) calculations that account for the extrapolation to the complete basis set limit and core correlation effects. A first important outcome is the definitive confirmation of the nonplanarity of carbamic acid, then followed by an accurate estimate of its rotational and vibrational spectroscopy parameters. As far as the carbamic acid dimer is concerned, the investigation started from the identification of its most stable forms. For them, structure and vibrational properties have been evaluated using density functional theory, while a composite scheme rooted in CC theory has been employed for the energetic characterization. Our results allowed us to provide a better interpretation of the feature observed in the recent experiment mentioned above.

KEYWORDS
carbamic acid, carbamic acid dimers, equilibrium structure, energetics, rotational spectroscopy, vibrational spectroscopy

1 | INTRODUCTION

Detection in the interstellar medium (ISM) of prebiotic molecules containing C, N, and O can provide important insights into elucidating the chemical evolution in space and its potential role in the origin of life. Among small prebiotic species, carbamic acid (H_2NCOOH) is the simplest species containing both the carboxyl (−COOH) and amino ($-NH_2$) groups, which is a characteristic it shares with amino acids. H_2NCOOH is considered the precursor of biologically significant species such as pyrimidine-derived nucleobases and amino acids.[1–4]

In the ISM, H_2NCOOH can be formed on grains in ammonia-carbon dioxide-rich (NH_3-CO_2) ices. Indeed, several experiments demonstrated that, in interstellar analog ices containing ammonia and carbon dioxide, thermal reactions and nonequilibrium processes induced by energetic particles (e.g., low-energy electrons), ultraviolet radiation or cosmic-ray proxies lead to the formation of carbamic acid and the ammonium carbamate salt (H_2NCOO^- NH_4^+).[5–18] However, carbamic acid turned out to be an elusive species because of its instability in such ionizing environments. Very recently, Marks et al.[18] demonstrated that heating of interstellar ice analogs composed of carbon dioxide and ammonia produces carbamic acid already at low temperatures (below 100 K) without the help of any energetic radiation, with ammonium carbamate starting to form even at lower temperatures. In Reference 18, a simultaneous analysis of the condensed and gas phases pointed out that H_2NCOOH is relatively stable in the latter while conducting temperature-programmed desorption (TPD) experiments. The greatest abundance of carbamic acid in the gas phase was found at 250 K in correspondence of the largest rate of decrease of the signal (in the infrared (IR) spectrum) of ammonium carbamate in the solid phase,[18] thus suggesting that sublimation of ammonium carbamate not only leads to its dissociation into its precursors, but also to a good fraction of H_2NCOOH. Since the thermal instability of this

latter is such that it spontaneously dissociates, at room temperature, into NH_3 and CO_2, the results of Reference 18 offer hope toward its spectroscopic characterization in the gas phase. Indeed, the authors suggested carbamic acid and the corresponding ammonium salt as potential candidates for astronomical observations in the gas and solid phases, respectively.[18] Interestingly, IR spectra recorded continuously during TPD showed the formation of a dimer of carbamic acid,[18] as already noted in some previous experiments.[6,8,17,19–21] Actually, in Reference 18, the fraction of carbamic acid that was found remaining in the ice above 250 K is in the form of its dimer. Density functional calculations of its vibrational spectrum at the harmonic level led to assign such a dimer to a centrosymmetric form with hydrogen bonds binding the carboxylic acid moieties.[18]

Spurred by the results obtained in Reference 18 and the lack of spectroscopic information for the isolated carbamic acid and its dimer, an accurate structural, energetic and spectroscopic characterization has been carried out. To the best of our knowledge, carbamic acid has never been characterized in the gas phase by any experimental technique, while its zwitterionic form ($^+H_3NCOO^-$) and ammonium carbamate have been identified by IR spectroscopy in the solid phase.[8,13–15,22] These experimental studies were often supported by calculations, which aimed at facilitating the spectral assignments, but employed very low levels of theory.[6,17,20] The only high-level structural determination of H_2NCOOH was carried out in Reference 23 where the equilibrium geometry was evaluated at different levels of theory ranging from density functional theory (DFT: B3LYP[24] in conjunction with cc-pVTZ[25]) to Møller–Plesset perturbation theory to second order (MP2[26]) in combination with cc-pVQZ,[25] to CCSD(T) (coupled-cluster singles doubles method with a perturbative treatment of triple excitations[27]) in conjunction with cc-pVTZ and aug-cc-pVTZ.[28] All the levels of theory considered pointed out the lack of planarity of H_2NCOOH.[23] As far as the carbamic acid dimer is concerned, a few works reporting its IR characterization in solid have been found in the literature.[6,8,17–21] However, only the centrosymmetric form mentioned above has been considered so far.

2 | METHODOLOGY

As mentioned in the Section 1, carbamic acid and its dimer have been investigated from a structural, energetic and spectroscopic point of view. Because of the different levels of knowledge available for the two systems as well as in view of the different dimensions (which strongly affect the computational cost), rather different methodologies have been employed. Therefore, in the following, they are presented separately.

All MP2 and CCSD(T) computations have been carried out with the CFOUR software.[29,30] All DFT calculations and single-point energies required within the so-called junChS composite scheme (*vide infra*) have been performed using the Gaussian suite of programs.[31] All DFT computations, even if not explicitly mentioned, incorporate dispersion (D3BJ) corrections.[32,33]

2.1 | Carbamic acid

Both the planar and nonplanar equilibrium structures of H_2NCOOH have been investigated at a high-level of theory in order to understand whether its peptide bond (also denoted as amide bond, –CO-NH-) is planar or not. In fact, the planarity of formamide (H_2NCOH) could be demonstrated only employing correlated methods in conjunction of quadruple-zeta basis sets.[34] In this work, the CCSD(T) method has been used, within the frozen-core (fc) approximation, in conjunction with the Dunning cc-pVTZ and cc-pVQZ sets, with the corresponding results extrapolated to the complete basis set (CBS) limit using the n^{-3} formula by Helgaker and co-workers.[35] Additionally, core-valence (CV) correlation effects have been incorporated using MP2 and the cc-pCVTZ basis set.[25,36] The resulting composite scheme is

$$r_{best} = r(\mathrm{CCSD(T)/CBS}) + \Delta r(\mathrm{MP2/CV}), \tag{1}$$

where r denotes a generic structural parameter and r(CCSD(T)/CBS) has been obtained as[37]

$$r(\mathrm{CCSD(T)/CBS}) = \frac{n^3 \times r(\mathrm{CCSD(T)/QZ}) - (n-1)^3 \times r(\mathrm{CCSD(T)/TZ})}{n^3 - (n-1)^3}, \tag{2}$$

where $n = 4$ and, thus, it corresponds to the fc-CCSD(T) calculation performed with the cc-pVQZ basis. Analogously, $n-1 = 3$ corresponds to the computation with cc-pVTZ. Clearly, r(CCSD(T)/QZ) and r(CCSD(T)/TZ) denote the values of the generic structural parameter optimized at the fc-CCSD(T)/cc-pVQZ and fc-CCSD(T)/cc-pVTZ levels, respectively. As demonstrated in Reference 37, application on empirical basis of Equation (2) to geometrical parameters provides results that negligibly differ from those theoretically sounded obtained from applying it to correlation energy followed by energy derivation (as done in Reference 38). The CV term has been derived as difference between geometry optimizations at the MP2/cc-pCVTZ level correlating all (all-MP2) and valence (fc-MP2) electrons:

$$\Delta r(\mathrm{MP2/CV}) = r(\mathrm{all\text{-}MP2/cc\text{-}pCVTZ}) - r(\mathrm{fc\text{-}MP2/cc\text{-}pCVTZ}). \tag{3}$$

Subsequently, on top of the best-estimated structures (hereafter denoted as CBS+CV(MP2)), the energy for both the planar and nonplanar species has been evaluated using a composite scheme entirely rooted in the coupled-cluster theory[39]:

$$E(\mathrm{CBS+CV}) = E(\mathrm{HF/CBS}) + \Delta E(\mathrm{CCSD(T)/CBS}) + \Delta E(\mathrm{CCSD(T)/CV}). \tag{4}$$

The first term on the right-hand side of the equation above accounts for the extrapolation to the CBS limit of the HF-SCF energy using the cc-pVnZ basis sets, with n = T, Q and 5, thereby exploiting the exponential extrapolative formula by Feller.[40] The second term is the extrapolation to CBS of the correlation CCSD(T) energy with the n^{-3}

expression in analogy to Equation (2). The last term incorporates the CV correction, which is evaluated as energy difference between all- and fc-CCSD(T) calculations in the same basis set (cc-pCVTZ).

To confirm the nature of the optimized structures (minimum or transition state), Hessian evaluations (i.e., harmonic force-field calculations) have been carried out on both planar and nonplanar geometries at the fc-CCSD(T)/cc-pVTZ, fc-MP2/cc-pVTZ, fc-MP2/cc-pVQZ, fc-MP2/cc-pCVTZ, and all-MP2/cc-pCVTZ levels of theory (also fc-CCSD(T)/cc-pVQZ for the planar structure). In addition to clarify the nature of the peptide bond (planar or not), such computations give access to vibrational frequencies (denoted as ω_i) within the harmonic-oscillator approximation in a normal mode representation. In this respect, the harmonic force-field calculations mentioned above allow for the exploiting the so-called cheap composite scheme (ChS)[41,42]:

$$\omega_i(\mathrm{ChS}) = \omega_i(\mathrm{CCSD(T)/TZ}) + \Delta\omega_i(\mathrm{MP2/CBS}) + \Delta\omega_i(\mathrm{MP2/CV}), \quad (5)$$

where $\omega_i(\mathrm{CCSD(T)/TZ})$ denotes the harmonic frequency of the generic i-th normal mode evaluated at the fc-CCSD(T)/cc-pVTZ level. The second and third terms on the right-hand side of the equation above indicate the correction due to extrapolation to CBS and the CV contribution, respectively, both of them obtained at the MP2 level in analogy to what done before for structural parameters. Straightforwardly, the composite scheme above allows for accurately deriving zero-point energy (ZPE) corrections, within the harmonic approximation, for the energetic investigation.

Combination of the harmonic force-field calculations presented above with anharmonic ones gives access to the evaluation of rotational and vibrational spectroscopic parameters. At this stage, only the nonplanar form has been considered because the planar one has been demonstrated to be a transition state. Concerning rotational spectroscopy, according to vibrational perturbation theory to second order (VPT2),[43] rotational constants consist of two terms:

$$B_0^i = B_e^i - \frac{1}{2}\sum_r d_r \alpha_r^i = B_e^i + \Delta B_{\mathrm{vib}}^i. \quad (6)$$

where B_e^i is the equilibrium rotational constant relative to the i-th inertial axis ($i = a$, b or c so that, e.g., $B^a = A$), which is straightforwardly derived from the equilibrium structure.[44–46] $\Delta B_{\mathrm{vib}}^i$ is the vibrational correction, which is obtained by summing, over all vibrational modes r (d_r being their degeneracy), the vibration-rotation interaction constants (α_r^i). Calculation of the latter parameters requires to apply VPT2 to a force field containing up to the cubic terms.[46–49] In details, anharmonic force-field computations have been carried out at the fc-MP2/cc-pVTZ level. The set of rotational parameters is complemented by the quartic centrifugal distortion constants obtained as a by-product of harmonic force-field calculations. Therefore, their best estimates could be obtained by exploiting the ChS composite scheme of Equation (5).

Moving to vibrational spectroscopy, from the inspection of the harmonic frequencies, carbamic acid is expected to present some singularities. To overcome the problems of perturbation theory related to them, a generalized VPT2 (GVPT2) approach has been employed,[50–53] which consists of removing the resonant terms from the perturbation treatment and then treating them with a proper reduced-dimensionality variational approach. To identify the resonances, the first-order derivatives of the harmonic frequencies have been inspected. For GVPT2, the GUINEA module of CFOUR has been used.[51–53] These GVPT2 computations provided anharmonic corrections ($\Delta\nu_i$) to harmonic frequencies, thus allowing to exploit a hybrid force-field approach.[39,42,54,55] Therefore, the MP2/cc-pVTZ anharmonic corrections have been applied to the best-estimated harmonic frequencies:

$$\nu_i = \omega_i(\mathrm{ChS}) + \Delta\nu_i(\mathrm{MP2/TZ}), \quad (7)$$

where $\Delta\nu_i$(MP2/TZ) is the anharmonic correction for the fundamental frequency of the ith normal mode, which is given by the difference between the anharmonic (ν_i) and harmonic frequency (ω_i) at the MP2/cc-pVTZ level. However, the lowest normal mode has been excluded from the treatment above because it is a large amplitude motion (LAM) and thus VPT2 is not applicable to it.

2.2 | Carbamic acid dimers

A preliminary investigation of carbamic acid dimers has been carried using the conformational search implemented in CREST[56,57] and employing as initial guess the structure of the dimer reported in Reference 18. This led to the discovery of four new dimers, which—together with the starting species—have been re-optimized using the double-hybrid rev-DSDPBEP86 functional[58] in conjunction with the jun-cc-pVTZ basis set[25,59] (this level of theory is hereafter denoted as revDSD/junTZ). To confirm that all the structures are minima, the corresponding Hessian has been computed at the same level, thereby obtaining as by-product the ZPE contribution, within the harmonic approximation, to energy and harmonic vibrational frequencies.

On top of the revDSD/junTZ geometries, for all dimers, the energy has been improved using the so-called junChS composite scheme,[60,61] which is a modification of the ChS approach (introduced in Equation 5) purposely set up for energetics. As suggested by the acronym, the junChS model employs the jun-cc-pVnZ basis sets.[25,59] Within such a composite scheme, the energy is given by

$$E(\mathrm{junChS}) = E(\mathrm{CCSD(T)/junTZ}) + \Delta E(\mathrm{MP2/CBS}) + \Delta E(\mathrm{MP2/CV}). \quad (8)$$

The first term on the right hand is the energy computed at the fc-CCSD(T)/jun-cc-pVTZ level. The second term represents the extrapolation to the CBS limit of the MP2 energy, using the formula of Equation (2) and the jun-cc-pVTZ and jun-cc-pVQZ basis sets. The last term is the CV contribution computed as in Equation (3) using the cc-pwCVTZ basis.[62] According to the literature,[60,61,63–65] the junChS energies are expected to provide energies with an accuracy of about 2 kJ/mol. These, augmented by the harmonic-ZPE contributions at

the revDSD/junTZ level of theory, have been used to evaluate the relative energy of the carbamic acid dimers (E_{rel}) with respect to the most stable species. To further confirm the accuracy of the junChS energies, a scheme analogous to that of Equation (1) has also been exploited, which required additional calculations at the fc-CCSD(T)/jun-cc-pVQZ level for the extrapolation to the CBS limit. In the following, the resulting model is denoted as junCBS+CV(MP2), where the prefix "jun" has been added to stress that the extrapolation to the CBS limit of fc-CCSD(T) energies has been performed using the jun-cc-pV*n*Z basis sets, with n=T,Q. The accuracy of the junCBS+CV(MP2) scheme is expected to be of about 1 kJ/mol.[61]

To estimate the stability of the dimers with respect to the isolated monomers, the interaction energy (E_{int}) and the dissociation energy (D_0) have been determined. In the evaluation of E_{int}, the basis set superposition error (BSSE) has been incorporated via counterpoise (CP) correction[66] (thus leading to CP-corrected interaction energy, E_{int}^{CP}) as follows:

$$E_{int}^{CP} = E(AB) - E^{AB,AB}(A) - E^{AB,AB}(B), \quad (9)$$

where $E(AB)$ is the junChS energy of the dimer. The $E^{AB,AB}(A)$ and $E^{AB,AB}(B)$ terms are the junChS energies of the two monomers (A and B) computed using the basis set of the dimer and the geometries they assume within the dimer (the superscript being "Geo, Basis," that is the indication of the geometry and of the basis set). In the present case, since the complex AB is a dimer, A = B. If the energy of the monomers is computed using the basis set of the monomer, the non-counterpoised (NCP) corrected energy (E_{int}^{NCP}) is obtained.

From E_{int}^{CP}, the equilibrium dissociation energy D_e can be easily derived by considering the deformation when moving from the isolated monomers to the dimer.[60] The deformation term (Δ_{def}) has been computed as

$$\Delta_{def} = E^{AB,A}(A) + E^{AB,B}(B) - 2E^{A,A}(A). \quad (10)$$

In the equation above, the superscript "Geo, Basis" notation is used. Therefore, $E^{AB,A}(A)$ and $E^{AB,B}(B)$ are the junChS energies of the monomers computed using their basis sets at the revDSD/junTZ geometry of the dimer, while $E^{A,A}(A)$ is the junChS energy of carbamic acid, at the revDSD/junTZ equilibrium geometry, using its basis set. By combining the E_{int}^{CP} and Δ_{def} contributions, D_e is thus obtained. Then, by incorporating Δ_{ZPE}, D_0 is derived as:

$$D_0 = -(\Delta_{def} + E_{int}^{CP}) + \Delta_{ZPE} = D_e + \Delta_{ZPE}. \quad (11)$$

The term denoted as Δ_{ZPE} is the difference between the harmonic-ZPE correction of the dimer and that of two monomers (i.e., two isolated carbamic acids), computed at the revDSD/junTZ level of theory.

For the dimers that are expected to be stable with respect to dissociation (i.e., positive values for D_0), the fundamental frequencies have been obtained by applying a hybrid scheme analogous to that of Equation (7). In detail, they have been calculated by correcting the revDSD/junTZ harmonic frequencies for the anharmonic contributions at the B3LYP/jun-cc-pVDZ level (hereafter B3LYP/junDZ). Since the dimers have very low-frequency vibrations due to large amplitude motions, the anharmonic corrections have been applied only to the vibrational modes lying above 400 cm^{-1} at the B3LYP/junDZ level.

3 | RESULTS AND DISCUSSION

As mentioned in the Section 1, the main aim of this work is to spectroscopically characterize carbamic acid and its dimers in view of supporting future experimental laboratory investigations. For both of them, the characterization lays its foundations in an accurate structural and energetic determination. In analogy to the Section 2, the presentation of the results and their discussion is reported separately for carbamic acid and its dimers.

3.1 | Carbamic acid

To proceed toward the spectroscopic characterization, the first issue to address is the planarity or not of carbamic acid. As summarized in the Introduction, in Reference 23, different levels of theory pointed out the lack of planarity of peptide bond. In this work, the planar and nonplanar structures have been optimized at different levels of theory: MP2 in conjunction with the cc-pVTZ, cc-pVQZ and cc-pCVTZ basis sets, within the fc approximation and correlating all electrons in the case of cc-pCVTZ; CCSD(T) in conjunction with the cc-pVTZ and cc-pVQZ basis sets, within the fc approximation. In all these cases, the planar species has been found to be a transition state (thus showing an imaginary vibrational frequency). The molecular structure of nonplanar carbamic acid is depicted in Figure 1, while—for both planar and nonplanar forms—the geometrical parameters are collected in Table 1, where the results from the CBS+CV(MP2) composite scheme (Equation 1) are also reported.

From the inspection of Table 1, the usual trend when enlarging the basis set is noted. Bond distances shorten by about 1–3 mÅ when moving from cc-pVTZ to cc-pVQZ and by about 0.5–2 mÅ when moving from cc-pVQZ to CBS, where the smaller values refer to the N-H and O-H bonds and the larger ones to the C-O and C-N distances. While for bond lengths the behaviors of the planar and nonplanar forms are very similar, when moving to angles, the modifications are more noticeable for the nonplanar species. For planar carbamic acid, corrections to angles are negative and smaller than 0.1 degrees, the only exception being the ∠HOC angle, whose variation is positive and of the order of 0.3–0.4 deg. For the nonplanar structure, changes in angles are either positive or negative, and appreciably larger (as large as ∼2 deg. for the ∠dH1 and ∠dH2 dihedral angles). Concerning the quality of the CBS+CV(MP2) structure, it is expected that its accuracy is similar to that of the CCSD(T)/CBS+CV one (entirely rooted in the CC theory) because MP2 is well suited for evaluating the CV correction. As well-known, the effect of correlating core electrons cannot be neglected when aiming at highly accurate equilibrium structures.[46,49,67] For the nonplanar geometry, its incorporation

FIGURE 1 Molecular structure of carbamic acid and atom labeling.

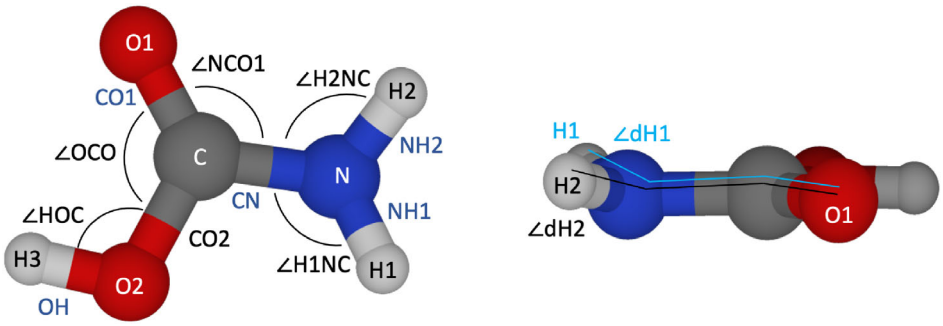

TABLE 1 Structural parameters of carbamic acid (planar and nonplanar), together with the corresponding equilibrium rotational constants.[a]

Parameter	CCSD(T)/VTZ	CCSD(T)/VQZ	CCSD(T)/CBS	ΔCV(MP2)	CBS+CV(MP2)	Reference 23[b]
Planar						
rCO1/Å	1.2108	1.2084	1.2067	−0.0017	1.2050	
rCO2/Å	1.3609	1.3572	1.3546	−0.0022	1.3524	
rCN/Å	1.3564	1.3534	1.3513	−0.0021	1.3492	
rNH1/Å	1.0011	1.0005	1.0000	−0.0009	0.9992	
rNH2/Å	1.0008	1.0002	0.9997	−0.0009	0.9988	
rOH/Å	0.9645	0.9629	0.9617	−0.0008	0.9609	
∠OCO/deg.	123.60	123.55	123.52	−0.03	123.49	
∠NCO1/deg.	126.00	125.92	125.86	−0.02	125.84	
∠H1NC/deg.	120.91	120.88	120.87	−0.00	120.87	
∠H2NC/deg.	118.28	118.27	118.27	−0.00	118.27	
∠HOC/deg.	104.63	105.07	105.39	0.09	105.48	
A_e/MHz	11,579.5	11,636.3	11,678.1	–	11,716.8	
B_e/MHz	10,884.4	10,921.3	10,948.2	–	10,976.5	
C_e/MHz	5610.6	5633.7	5650.7	–	5667.3	
Nonplanar						
rCO1/Å	1.2097	1.2076	1.2061	−0.0015	1.2045	1.2076
rCO2/Å	1.3594	1.3563	1.3541	−0.0021	1.3520	1.3547
rCN/Å	1.3658	1.3602	1.3561	−0.0030	1.3531	1.3577
rNH1/Å	1.0041	1.0026	1.0015	−0.0011	1.0004	1.0020
rNH2/Å	1.0037	1.0022	1.0012	−0.0011	1.0000	1.0014
rOH/Å	0.9647	0.9630	0.9618	−0.0008	0.9610	0.9634
∠OCO/deg.	123.65	123.58	123.52	−0.03	123.49	123.70
∠NCO1/deg.	125.90	125.84	125.80	−0.01	125.79	125.86
∠H1NC/deg.	117.79	118.60	119.19	0.28	119.47	118.85
∠H2NC/deg.	115.33	116.14	116.73	0.27	117.01	116.38
∠HOC/deg.	104.78	105.17	105.45	0.08	105.53	105.43
∠dH1/deg.	162.87	165.40	167.26	0.89	168.15	166.18
∠dH2/deg.	16.93	14.70	13.07	−0.91	12.16	14.00
∠dN[c]/deg.	177.79	178.07	178.28	0.14	178.42	178.75
∠dOH[d]/deg.	0.36	0.40	0.44	0.00	0.44	0.28
A_e/MHz	11,577.0	11,635.9	11,679.6	–	11,718.5	
B_e/MHz	10,839.6	10,887.3	10,921.2	–	10,953.4	
C_e/MHz	5611.9	5634.7	5651.7	–	5668.3	

[a]For the atom labeling, the reader is referred to Figure 1.
[b]At the fc-CCSD(T)/aug-cc-pVTZ level.
[c]∠NCOH (NCO2H3) dihedral angle.
[d]∠OCOH (O1CO2H3) dihedral angle.

decreases the bond lengths by 1–2 mÅ, and similar is the behavior for the planar species. As noted for the CBS corrections, there is not systematic trend for angles for the nonplanar form, with corrections that can be as large as 0.9 deg (again for the ∠dH1 and ∠dH2 dihedral angles). In analogy to CBS, for the planar structure, corrections are negative with the exception of the ∠HOC angle. Overall, the accuracy of the CBS+CV(MP2) geometry can be estimated to be 0.001–0.002 Å for bond distances and 0.1 deg. for angles.[39,68–70]

As evident from Figure 1 and Table 1, nonplanarity is due to the $-NH_2$ moiety having the nitrogen atom with a slight pyramidal structure and the two hydrogens thus lying out of the molecular plane. The computed dihedral angles deviate from planarity by a bit more than 15 degrees. As a consequence, also the ∠NCOH dihedral angle little deviates from the planarity (by about 2 deg.), while the deviation for the ∠OCOH dihedral angle is almost negligible (∼0.4 deg.). As noted in Reference 23, the dihedral angles involving the NH frame show considerable variations by varying the level of theory. As mentioned above, imposing the constraint of planarity in the geometry optimization procedure always led to one imaginary vibrational frequency. However, the energy difference between the planar and nonplanar forms is rather small. In Reference 23, differences of only 20–30 cm^{-1} are mentioned for CCSD(T) calculations in conjunction with the cc-pVTZ and aug-cc-pVTZ basis sets, with all electrons correlated. These can be compared with our results that are reported in Table 2. It is noted that the energy difference reduces by enlarging the basis set and incorporating the CV correction. Our best estimate is the CCSD(T)/CBS+CV value obtained by exploiting the composite scheme introduced in Equation (4), 14.2 cm^{-1} (0.17 kJ/mol), which is in line with what determined in Reference 23. From the inspection of Table 2, it is observed that, once the harmonic-ZPE correction is incorporated, the planar structure becomes more stable by about 79 cm^{-1} (∼ 1 kJ/mol). However, it has to be noted that all these values are smaller than the expected uncertainty affecting the CCSD(T)/CBS+CV model, which is estimated of the order of 1 kJ/mol.[39,71] Table 2 also reports the result from the CBS+CV(MP2) composite scheme (used for the structural determination), which does not consider the separated extrapolation of the HF-SCF and CCSD(T) correlation energies (as in Equation 4) and incorporates the CV correction at the MP2 level. Despite the reduction in the level of theory, the CBS+CV(MP2) relative energy differs only by less than 0.1 kJ/mol from the more accurate CCSD(T)/CBS+CV result.

Since the planar form of carbamic acid has been found to be a transition state, the spectroscopic characterization has been carried out only for the nonplanar species. Its computed rotational and quartic centrifugal parameters are collected in Table 3. The rotational constants have been obtained by combining the CBS+CV(MP2) equilibrium rotational constants (reported in Table 1) with the fc-MP2/cc-pVTZ vibrational corrections. The quartic centrifugal distortion constants have instead been evaluated by applying the ChS model (Equation 5) to centrifugal distortion constants. The dipole moment components along the inertial axes are also given. Based on the quality of the CBS+CV(MP2) structure, for rotational constants, we expect an accuracy of about 0.2%–0.3%.[49] As far as centrifugal parameters are concerned, the exploitation of a composite scheme that incorporates corrections accounting for the extrapolation to the

TABLE 3 Computed rotational and centrifugal distortion[a] constants of carbamic acid.

Constant	Unit	
A_0	MHz	11,643.6
B_0	MHz	10,923.7
C_0	MHz	5619.8
Δ_J	kHz	5.63
Δ_{JK}	kHz	−2.42
Δ_K	kHz	8.93
δ_J	kHz	2.42
δ_K	kHz	5.09
μ_a[b]	D	−1.52
μ_b[b]	D	1.87
μ_c[b]	D	0.53

[a]Rotational constants: CBS+CV(MP2) equilibrium rotational constants augmented by fc-MP2/cc-pVTZ vibrational corrections. Quartic centrifugal distortion constants evaluated using the ChS composite scheme (Equation 5). Watson A-reduction in the I^r representation has been used.
[b]At the fc-CCSD(T)/cc-pVQZ level augmented for the effect of diffuse functions at the MP2 level. See text.

TABLE 2 Energy difference[a] for planar-nonplanar carbamic acid.

	Unit	CCSD(T)/VTZ	CCSD(T)/VQZ	CCSD(T)/CBS	CCSD(T)/CBS+CV	CBS+CV(MP2)[b]
ΔE[c]	kJ/mol	0.82	0.46	0.24	0.17	0.09
ΔE[c]	cm^{-1}	68.24	38.65	20.06	14.15	7.83
ΔE_0[d]	kJ/mol	−0.30	−0.66	−0.88	−0.95	−1.02
ΔE_0[d]	cm^{-1}	−25.22	−54.82	−73.41	−79.32	−85.64

[a]Difference between the energy of the planar structure and that of the nonplanar one. At the CCSD(T)/CBS+CV level, electronic energy is −245.13801247 E_h and −245.13804198 E_h for the of the planar and nonplanar form, respectively.
[b]Relative energies as obtained from the application of the composite scheme of Equation (1).
[c]Relative energies (ΔE) on top of the CBS+CV(MP2) equilibrium geometries (Equation 1).
[d]ΔE incorporating harmonic ChS ZPE corrections. ChS ZPE values (composite scheme of Equation (5)) are: 134.15 kJ/mol for the planar species, 135.27 kJ/mol for the nonplanar species.

CBS limit and CV effects on top of fc-CCSD(T)/cc-pVTZ calculations leads to quartic terms determined with an accuracy of about 1%.[41] Finally, the values of the dipole moment components reported in Table 3 surely provide good estimates (more than semi-quantitative), which are suitable for predicting the intensity of the rotational transitions. Indeed, dipole moment components have been obtained by incorporating in the fc-CCSD(T)/cc-pVQZ values the effect of diffuse functions, which are known to be important for this property,[46,72,73] thus leading to estimates with an accuracy of 0.5%–2%. The contribution of diffuse functions has been derived as difference between fc-MP2 computations performed in conjunction with the aug-cc-pVTZ and cc-pVTZ basis sets. According to the estimated dipole moment components, rotational spectrum of carbamic acid is characterized by intense *a*- and *b*-type transitions and rather weak *c*-type ones.[44]

Calculation of harmonic and anharmonic force fields gives access to all information required for the prediction of the vibrational IR spectrum. As explained in the Section 2, our best estimates have been obtained by combining the harmonic wavenumbers at the ChS level with anharmonic corrections at the fc-MP2/cc-pVTZ level. The corresponding results for fundamental transitions are reported in Table 4. This table also collects harmonic vibrational wavenumbers from the different contributions to the ChS approach: the values at the fc-CCSD(T)/cc-pVTZ level and the MP2/CBS and MP2/CV corrections. It is first of all noted that the CBS correction is not systematic as it might either increase or decrease the fc-CCSD(T)/cc-pVTZ value and its magnitude ranges from being negligible (e.g. +0.5 cm^{-1} for ν_7) up to ~8 cm^{-1} (for ν_2 and ν_{14}), with only two exceptions. These are ν_1, the NH_2 wagging mode, which shows a large decrease by about 87 cm^{-1}, and ν_{12}, the C=O stretching, whose correction is nearly −21 cm^{-1}. CV contributions are instead always positive and, on average, smaller than the corresponding CBS corrections. The only exception is again noticed for ν_1, the corresponding CV contribution being about −21 cm^{-1}. The first conclusion is that the harmonic frequency of the LAM is very sensitive to the level of theory employed for its calculation. At the MP2 level, moving from cc-pVTZ to cc-pVQZ decreases the value by about 50 cm^{-1} and from cc-pVQZ to CBS by about 37 cm^{-1}, thus giving to an overall CBS correction of about −87 cm^{-1}. Using the cc-pVTZ set, going from MP2 to CCSD(T) increases the ν_1 harmonic frequency by about 12 cm^{-1}. On the basis of the approximations made, the corrections included, and the literature on this topic (see, e.g., References 42, 55, and 74), we expect an accuracy for the ChS harmonic frequencies of a few wavenumbers (from 5 to 10 cm^{-1}) for all modes but ν_1. For the latter, a conservative uncertainty is estimated to be about 20 cm^{-1}. Anharmonic corrections are a few percents of the harmonic frequencies. Therefore, their uncertainties have a very small impact on the final accuracy of computed fundamentals. Conservatively, the accuracy of these latter (from the hybrid scheme) is about 6–11 cm^{-1}.[42] From the inspection of the harmonic IR intensities, the strongest bands are those lying in the 1200–1900 cm^{-1} range, with ν_{12} being by far the most intense.

3.2 | Carbamic acid dimers

The preliminary investigation pointed out the existence of five dimers of carbamic acid within a 100 kJ/mol threshold. These are

TABLE 4 Harmonic vibrational wavenumbers ω (cm^{-1}), harmonic infrared intensities I_{IR} (km/mol), anharmonic corrections $\Delta\nu$ (cm^{-1}), and hybrid fundamental wavenumbers ν (cm^{-1}) of carbamic acid.

	ω				I_{IR}	$\Delta\nu$[a]	Hybrid ν[b]
	CC/TZ[c]	ΔCBS	ΔCV	ChS	ChS	MP2/VTZ	
ν_1	349.9	−87.0	−20.8	242.1	226.5	—[d]	242.1
ν_2	462.8	8.0	2.5	473.4	37.2	0.1	473.5
ν_3	496.5	1.2	1.0	498.8	20.6	−18.7	480.1
ν_4	572.7	5.2	2.2	580.1	71.7	−9.1	571.0
ν_5	589.7	2.3	1.8	593.9	30.8	−13.4	580.4
ν_6	786.7	1.1	3.1	790.9	27.1	−3.5	787.4
ν_7	964.1	0.5	3.0	967.6	41.3	−45.1	922.5
ν_8	1098.6	−3.6	0.8	1095.8	54.5	−41.3	1054.5
ν_9	1250.4	−4.5	0.6	1246.4	179.9	−53.1	1193.3
ν_{10}	1449.0	−7.3	4.0	1445.7	130.0	−35.0	1410.7
ν_{11}	1630.3	−4.8	1.2	1626.7	111.8	−72.4	1554.3
ν_{12}	1853.8	−21.2	4.5	1837.1	538.2	−35.8	1801.3
ν_{13}	3629.9	4.6	7.7	3642.1	58.9	−125.3	3516.8
ν_{14}	3759.9	8.0	8.7	3776.6	71.5	−132.1	3644.5
ν_{15}	3822.8	1.3	5.7	3829.9	96.5	−179.3	3650.6

[a]From GVPT2 analysis using the fc-MP2/cc-pVTZ anharmonic force field. See text.
[b]Harmonic ChS wavenumbers (see, Equation 5) a posteriori corrected for anharmonic contributions at the fc-MP2/cc-pVTZ level. See text.
[c]CC/TZ stands for fc-CCSD(T)/cc-pVTZ.
[d]Normal mode excluded from the VPT2 treatment. See text.

sketched in Figure 2 and labeled according to their relative energy with respect to the most stable form (dimer 1). As explained in the Methodology section, energetics has been evaluated at the junChS and junCBS+CV(MP2) levels and incorporates harmonic revDSD/junTZ ZPE correction. The results are summarized in Table 5. From the inspection of this table, it is first of all noted that the junChS and junCBS+CV(MP2) values agree well within 1 kJ/mol. Therefore, their expected accuracy of 2 kJ/mol and 1 kJ/mol (see Section 2), respectively, is somewhat confirmed. It is observed that, at the junCBS+CV(MP2) level, CP and NCP interaction energies agree within 0.1 kJ/mol, thus confirming that the extrapolation of fc-CCSD(T)/jun-cc-pVTZ and fc-CCSD(T)/jun-cc-pVQZ energies correctly gives the fc-CCSD(T)/CBS result, the BSSE vanishing by definition at the CBS limit. For junChS, the CP-NCP difference ranges between 0.5 and 1 kJ/mol; this points out that, as expected, the reduced accuracy when moving from junCBS+CV to junChS is due to the approximation introduced in the latter for estimating the CCSD(T)/CBS limit, while MP2 is well suited for evaluating the CV correction. We can thus conclude that using the first two terms of Equation (8), i.e. combining the fc-CCSD(T)/jun-cc-pVTZ energy and the MP2/CBS correction, leads to an error of about 1 kJ/mol in approximating the fc-CCSD(T)/CBS result.

As noted in Figure 2, all dimers are characterized by two hydrogen bonds (HBs), where the proton donor is either the OH or the NH_2 group, while the proton acceptor is typically either the oxygen atom of the C=O bond or oxygen of the OH moiety. In dimer 1, that is, the species observed in Reference 18, two identical HBs are present, both of them involving the OH terminal of one monomer as proton donor and the C=O group of the other monomer as proton acceptor. The two COOH moieties are nearly on the same plane, while the

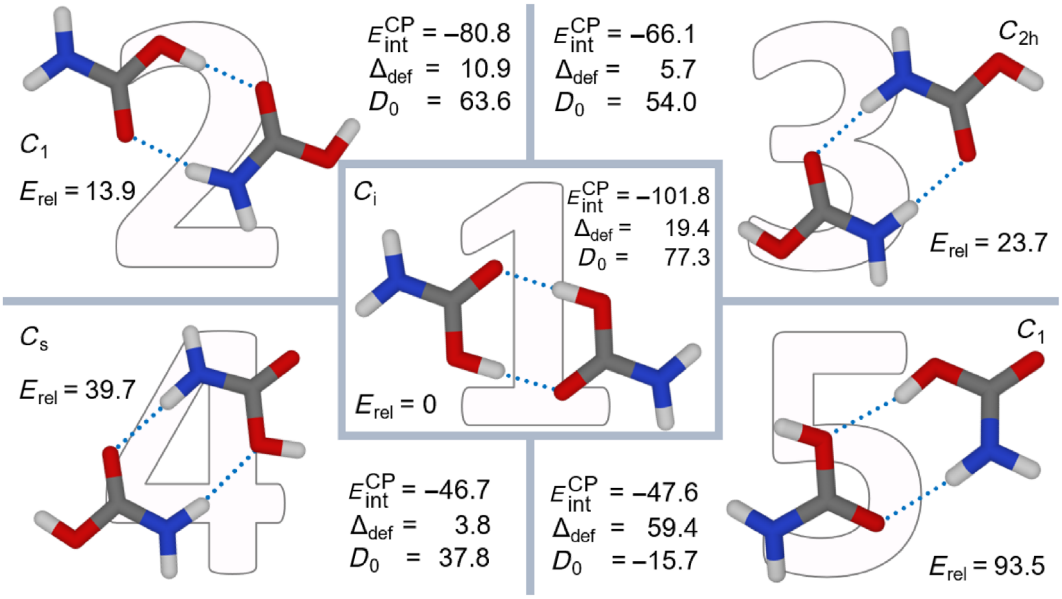

FIGURE 2 The five dimers of carbamic acid considered in this study together with their energetic quantities (kJ mol^{-1}) at the junChS level. For their definition, see text.

TABLE 5 Energetic properties (kJ/mol) of carbamic acid dimers.

	Dimer 1		Dimer 2		Dimer 3		Dimer 4		Dimer 5	
	junChS	CBS+CV[a]	junChS	CBS+CV[a]	junChS	CBS+CV[a]	junChS	CBS+CV[a]	junChS	CBS+CV[a]
E_{int}^{CP}	−101.8	−102.9	−80.8	−81.6	−66.1	−66.8	−46.7	−47.2	−47.6	−48.1
E_{int}^{NCP}	−102.9	−102.9	−81.6	−81.5	−66.7	−66.7	−47.2	−47.1	−48.1	−48.0
Δ_{def}	19.4	19.3	10.9	10.8	5.7	5.7	3.8	3.8	59.4	59.7
D_e	82.4	83.5	69.9	70.8	60.4	61.1	42.9	43.4	−11.8	−11.7
D_0[b]	77.3	78.4	63.6	64.5	54.0	54.7	37.8	38.3	−15.7	−15.6
E_{rel}^{eq}	0.0	0.0	12.8	12.8	22.5	22.5	40.0	40.2	94.8	95.3
E_{rel}^{0}[b]	0.0	0.0	13.9	13.9	23.7	23.7	39.7	39.8	93.5	94.0

[a]CBS+CV stands for junCBS+CV(MP2). See text.
[b]ZPE at the revDSD/junTZ level within the harmonic approximation. See text.

hydrogens of the NH_2 groups lie out of plane. Since the H atoms of a given monomer point in the same direction but the hydrogens belonging to different monomers are in opposite direction, dimer 1 has C_i symmetry. Our study confirms that dimer 1 is the most stable form and has the strongest interaction energy between the two monomers, that is, −102/−103 kJ/mol (depending on the level of theory considered; see Table 5). The deformation associated to the transition from isolated monomers to the complex is about 19 kJ/mol, thus leading to a dissociation energy D_0 of 77–78 kJ/mol (see Table 5). The second dimer in the stability order (dimer 2) has C_1 symmetry and it is characterized by two different HBs: a carbamic acid unit donates a proton to the other carbamic acid via the OH···O=C interaction, while the other monomer establishes an interaction between its amine group and the C=O moiety of the initial monomer. Dimer 2 is about 14 kJ/mol less stable than dimer 1, with an interaction energy of about −81 kJ/mol, still pointing to a strong noncovalent interaction. In dimer 2, the deformation energy is less pronounced, ∼11 kJ/mol, with a resulting D_0 of about 64 kJ/mol. The slightly lower stability of dimer 2 with respect to dimer 1 is related to lower strength of the intermolecular bonds. This is also reflected in the value of the intermolecular angles: the closer to linearity, the stronger the interaction. For dimer 1, for symmetry reasons, the two intermolecular angles are equal one to the other, and their value is 178.6°. For dimer 2, the two angles are different: ∠O-H···O is 174.7° and ∠N-H···O 166.2°, thus deviating from linearity more than the intermolecular angles of dimer 1.

Moving to dimer 3, the two HBs are identical and involve the NH_2 group on one side and the carboxyl end on the other. Since the NH_2 moieties are involved in HBs, their hydrogens are forced to lie on the plane formed by carbamic acid skeleton. This dimer is planar and has an inversion center, thus it belongs to the C_{2h} point group. Its dissociation energy D_0 is about 54.0 kJ/mol; thus, it is stable with respect to dissociation into monomers and it contain strong HBs. The D_0 values of dimers 4 and 5 are about 38 and −16 kJ/mol, respectively, and their relative stability with respect to dimer 1 is 40 and 95 kJ/mol, respectively. Dimer 4 (still being planar) differs from dimer 3 for one HB, which—in the former—involves the oxygen atom of the OH group as acceptor instead of oxygen of the the C=O group as in dimer 3. Therefore, dimer 4 no longer has an inversion center; its point group symmetry is C_s. Such a modification in the HBs (going from dimer 3 to 4) accounts for a difference of 20 kJ/mol in the interaction energy and of about 5° in the intermolecular angle. Dimer 5 is the only complex here considered having a negative dissociation energy, which means that it is unstable with respect to the isolated monomers, even if the interaction energy is about −48 kJ/mol and the species lies within the 100 kJ/mol threshold above dimer 1. Such instability is due to the deformation term which is about 60 kJ/mol and is further increased by the inclusion of the harmonic ZPE. However, this form could still be present in the experiment of Reference 18 because in the solid phase, and more precisely in NH_3-CO_2 ices, other HBs might be established, thus stabilizing the cluster. Supporting Information Data S1 collects the revDSD/junTZ results together with the Cartesian coordinates of each dimer. Finally, it is noted that the HBs occurring in the two most stable carbamic acid dimers are comparable with those of formic acid (HCOOH, $\Delta E = 55.8$ kJ/mol),[75] acetic acid (CH_3COOH, $E_{int} = -80.8$ kJ/mol),[76] and formamide ($HCONH_2$, $\Delta E = -61.6$ kJ/mol).[34]

As the dimer of carbamic acid was observed in Reference 18 owing to one of its vibrational features, in Table 6, we report an improved estimate of the fundamental wavenumbers of dimer 1 and compare them with the harmonic values used in Reference 18. Since dimer 1 is the most stable and it was assumed to be the complex identified in Reference 18, here, we focus only on it; however, the results for the other dimers considered in this study are collected in the Supporting Information Data S1. In detail, in Table 6, our hybrid anharmonic and harmonic revDSD/junTZ wavenumbers are compared with the harmonic results from Reference 18 which were obtained using B3LYP in conjunction with the cc-pVTZ basis set. From this comparison, it is evident that some of the vibrational bands predicted in the literature as "very-weak" in intensity are actually non-active in the IR due to the C_i symmetry of the dimer. As additional comment, we note that there is an overall good agreement between our revDSD/junTZ harmonic frequencies and those at the B3LYP/cc-pVTZ level from Reference 18, with differences usually within 10 cm^{-1}. However, there are a few exceptions. For low-frequency modes (below 200 cm^{-1}), B3LYP seems to underestimate the transition frequencies, also affecting the mode order. While it is not surprising that revDSD/junTZ is able to better describe LAMs, the underestimation by about 100 and 90 cm^{-1} for ν_{31} and ν_{32} shown by B3LYP points out some limitation of the latter in accurate structural descriptions. This is further confirmed by the nonzero B3LYP intensities for those modes that, for symmetry reasons, should be IR-inactive. According to the literature on this topic (see, e.g., References 48 and 77), a hybrid force field combining the harmonic part from a double-hybrid functional calculation using a triple-zeta basis set with the anharmonic part obtained employing a global-hybrid functional in conjunction with a double-zeta basis provides fundamental frequencies with an average accuracy of about 8 cm^{-1} and maximum deviations of 13–15 cm^{-1}. However, these benchmark results have been obtained for isolated molecules. Therefore, a conservative deterioration of such an accuracy is here considered: an average error of 15 cm^{-1} is assumed, with maximum deviations within 20 cm^{-1}.

The vibrational mode assigned to the carbamic acid dimer in the experiment of Reference 18 is located in the 1210-1320 cm^{-1} range, peaking at 1247 cm^{-1}. For dimer 1, our calculations indicate the ν_{23} mode as the closest vibrational transition in this range, which is located at 1387 cm^{-1} at the harmonic level and shifts to 1365 cm^{-1} when incorporating the anharmonic contribution. This mode is the symmetric in-plane bending of the OH moieties and, according to the symmetry of dimer 1 (which has an inversion center), is IR-inactive. However, ν_{24}, which is the asymmetric in-plane bending of the OH moieties (and thus IR active), lies only ∼2 cm^{-1} higher in frequency (when anharmonicity is incorporated) and it is a very intense band. As can be noted in the Supporting Information Data S1, for dimers 2, 3 and 4, the ν_{23} and ν_{24} bands lie around 1200 $^{-1}$ (with ν_{24} being IR-inactive for dimer 3), with the only exception of the ν_{24} of dimer 2, whose frequency is about 1319 cm^{-1}. Therefore, the band observed in Reference 18 could be likely due to a mixture of

TABLE 6 Harmonic revDSD/junTZ vibrational wavenumbers ω (cm^{-1}), harmonic infrared intensities I_{IR} (km/mol), and hybrid fundamental wavenumbers ν (cm^{-1}) of dimer 1.

	This work			Literature[a]			This work			Literature[a]	
	ω	I_{IR}	Hybrid ν[b]	ω	I_{IR}		ω	Intensity	Hybrid ν[b]	ω	Intensity
ν_1	50.00	6.9	–	50.89	1.45	ν_{19}	1018.67	25.3	991.24	1013.54	22.08
ν_2	67.80	3.9	–	67.75	1.14	ν_{20}	1029.05	–	923.99	1023.24	0.07
ν_3	112.06	–	–	97.12	17.04	ν_{21}	1111.49	–	1083.00	1100.70	0.01
ν_4	166.22	–	–	113.67	413.64	ν_{22}	1115.11	20.6	987.47	1105.17	15.26
ν_5	186.97	0.1	–	114.25	2.74	ν_{23}	1387.58	–	1365.93	1380.23	0.001
ν_6	188.21	439.9	–	172.06	0.39	ν_{24}	1393.06	598.3	1367.76	1388.47	608.79
ν_7	197.81	0.0	–	198.30	0.36	ν_{25}	1514.43	154.8	1458.75	1506.77	125.19
ν_8	210.36	65.4	–	211.69	48.42	ν_{26}	1533.51	–	1426.26	1527.86	0.04
ν_9	506.81	–	466.84	507.65	0.0008	ν_{27}	1614.39	–	1550.86	1600.05	0.56
ν_{10}	540.54	41.0	912.44	545.59	44.21	ν_{28}	1637.32	376.0	1580.71	1623.79	382.56
ν_{11}	555.72	–	689.28	557.98	0.30	ν_{29}	1743.38	–	1697.63	1727.08	0.10
ν_{12}	565.79	28.5	255.57	560.75	29.07	ν_{30}	1772.76	1302.3	1712.41	1758.83	1246.38
ν_{13}	636.44	–	607.86	636.52	0.02	ν_{31}	3036.13	–	2422.10	2934.24	0.00
ν_{14}	652.87	27.7	653.71	655.63	22.56	ν_{32}	3150.91	3767.8	2579.52	3062.43	3909.37
ν_{15}	797.53	–	796.49	791.73	0.01	ν_{33}	3639.53	–	3567.44	3621.29	96.05
ν_{16}	798.48	14.2	798.38	793.49	15.96	ν_{34}	3639.94	–	3568.62	3621.66	0.55
ν_{17}	954.04	–	930.27	952.99	0.01	ν_{35}	3779.10	0.2	3734.35	3755.80	0.00
ν_{18}	993.06	164.9	991.81	994.94	178.02	ν_{36}	3779.16	140.3	3735.33	3755.86	124.73

[a]Reference 18: values computed at the B3LYP/cc-pVTZ level.
[b]Harmonic revDSD/junTZ vibrational wavenumbers augmented by anharmonic corrections at the B3LYP/junDZ level.

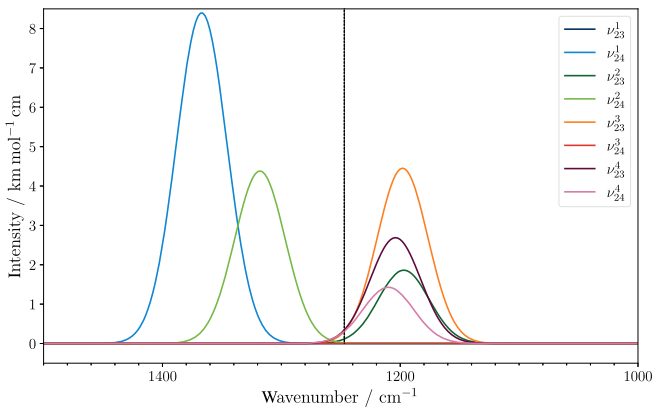

FIGURE 3 Plot of the ν_{23} and ν_{24} fundamental bands of the four most stable carbamic acid dimers (their labeling is reported as superscript): the transition lines have been convoluted with a Gaussian function with a half-width at half-maximum of 50 cm^{-1}. For the IR-inactive bands (ν_{23}^1 and ν_{24}^3), a very low intensity (1×10^{-4} km/mol) was employed, which still renders the bands not visible. The vertical bar denotes the position of the experimental feature of Reference 18.

different dimer structures, all contributing to the signal as shown in Figure 3. This figure provides a simulation of the 1000–1500 cm^{-1} portion of IR spectra overlapping the contributions due to the ν_{23} and ν_{24} bands of the four most stable dimers. The feature of Reference 18 has been recorded at 280 K; however, in our figure, the transitions belonging to the different dimers have not been weighted according to the Boltzmann distribution of population at that temperature because we assumed that, in the ice, geometries imposed by the solid state might also lead to the formation of the less stable dimers. Furthermore, it should be pointed out that our data have been obtained for isolated dimers, and thus could be rigorously compared only with gas-phase experiments. Conversely, the dimers formed in NH_3-CO_2 ices (as in the case of Reference 18) are expected to present IR features that are affected by noncovalent interactionswith the solid-ice matrix. These can surely have an impact on both the band center and the transition intensity. For example, shifts in frequency might occur thus leading to a more compact distribution of the vibrational features with respect to that of Figure 3.

4 | CONCLUDING REMARKS

A state-of-the-art quantum-chemical study has been performed to characterize the structure, energetics and spectroscopy of carbamic acid. Differently from formamide which only differs from the title molecule for a hydrogen in the place of the OH group, this molecule has been found to be nonplanar at all levels of theory considered. However, the energy difference with respect to the planar form is only

about 14 cm^{-1}. Furthermore, incorporation of harmonic-ZPE leads to a stabilization of the planar structure (which is the transition state along the NH_2 inversion motion) with respect to the nonplanar one. Therefore, on the vibrational ground state the molecule appears to be planar. Indeed, the deviation from planarity is so small that, at all levels of theory, the A_e and C_e constants of the planar and nonplanar species agree within 1 MHz, with only the B_e values differing by about 25 MHz. Furthermore, for the nonplanar form, both equilibrium and ground-state rotational constants lead to inertial defect of the order of 10^{-7} amuÅ^2. This work also provides the first accurate prediction of the rotational and vibrational spectroscopy parameters in the gas phase. Rotational and quartic centrifugal distortion constants are expected to have a relative accuracy of 0.2%–0.3% and 1%, respectively, thus providing good estimates for guiding future experimental investigations. Moving to vibrational spectroscopy, despite the presence of a LAM, the fundamental frequencies have been predicted with an accuracy of about 1%–2%, which is suitable for supporting experiment.

To the best of our knowledge, for the first time, an accurate investigation of the dimers formed by carbamic acid has been carried out. It has been found that, in addition to the symmetric dimer 1 considered in several previous works, other three dimers are stable with respect to dissociation, while the fifth one in the stability order is unstable. For all these five dimers, the geometry has been optimized using a double-hybrid density functional in conjunction with a partially augmented triple-zeta basis set. This level of theory, which has also been used for harmonic frequency calculations, is expected to provide equilibrium structures with an accuracy better than that obtainable from fc-CCSD(T)/cc-pVTZ computations.[48,77–79] Indeed, the accuracy of revDSD/junTZ bond distances and angles is predicted to be 3–4 mÅ and 0.3 deg., respectively. For the four dimers stable with respect to dissociation, revDSD/junTZ harmonic frequencies have been augmented by B3LYP/junDZ anharmonic corrections, thus allowing the prediction of their fundamental bands (non LAM) with an average accuracy of 20 cm^{-1} or better.[48]

ACKNOWLEDGMENTS

This work has been supported by MUR (PRIN Grant Number 202082CE3T) and by the University of Bologna (RFO funds). The COST Action CA21101 'COSY-Confined molecular systems: from a new generation of materials to the stars' is also acknowledged.

CONFLICT OF INTEREST STATEMENT

The authors declare no competing financial interest.

DATA AVAILABILITY STATEMENT

The data that support the findings of this study are available from the corresponding author upon reasonable request.

ORCID

Cristina Puzzarini https://orcid.org/0000-0002-2395-8532

REFERENCES

[1] W. W. Cleland, T. J. Andrews, S. Gutteridge, F. C. Hartman, G. H. Lorimer, *Chem. Rev.* **1998**, *98*, 549.
[2] C. Alcántara, J. Cervera, V. Rubio, *FEBS Lett.* **2000**, *484*, 261.
[3] D. B. Dell'Amico, F. Calderazzo, L. Labella, F. Marchetti, G. Pampaloni, *Chem. Rev.* **2003**, *103*, 3857.
[4] M. Moison, A. Marmagne, S. Dinant, F. Soulay, M. Azzopardi, J. Lothier, S. Citerne, H. Morin, N. Legay, F. Chardon, J.-C. Avice, M. Reisdorf-Cren, C. Masclaux-Daubresse, *J. Exp. Bot.* **2018**, *69*, 4379.
[5] S. Esmaili, A. D. Bass, P. Cloutier, L. Sanche, M. A. Huels, *J. Chem. Phys.* **2018**, *148*, 164702.
[6] Y. Rodríguez-Lazcano, B. Maté, V. J. Herrero, R. Escribano, O. Gálvez, *Phys. Chem. Chem. Phys.* **2014**, *16*, 3371.
[7] V. Vinogradoff, F. Duvernay, N. Fray, M. Bouilloud, T. Chiavassa, H. Cottin, *Astrophys. J. Lett.* **2015**, *809*, L18.
[8] X. Y. Lv, P. Boduch, J. J. Ding, A. Domaracka, T. Langlinay, M. E. Palumbo, H. Rothard, G. Strazzulla, *Phys. Chem. Chem. Phys.* **2014**, *16*, 3433.
[9] G. M. Muñoz Caro, W. A. Schutte, *Astron. Astrophys.* **2003**, *412*, 121.
[10] V. Vinogradoff, F. Duvernay, G. Danger, P. Theulé, T. Chiavassa, *Astron. Astrophys.* **2011**, *530*, A128.
[11] M. Bertin, I. Martin, F. Duvernay, P. Theule, J. B. Bossa, F. Borget, E. Illenberger, A. Lafosse, T. Chiavassa, R. Azria, *Phys. Chem. Chem. Phys.* **1838**, *2009*, 11.
[12] J. B. Bossa, P. Theulé, F. Duvernay, F. Borget, T. Chiavassa, *Astron. Astrophys.* **2008**, *492*, 719.
[13] D. L. Frasco, *J. Chem. Phys.* **1964**, *41*, 2134.
[14] C. Hisatsune, *Can. J. Chem.* **1984**, *62*, 945.
[15] R. Khanna, M. Moore, *Spectrochim. Acta A* **1999**, *55*, 961.
[16] Y. J. Chen, M. Nuevo, J. M. Hsieh, T. S. Yih, W. H. Sun, W. H. Ip, H. S. Fung, S. Y. Chiang, Y. Y. Lee, J. M. Chen, C. Y. R. Wu, *Astron. Astrophys.* **2007**, *464*, 253.
[17] Z. Altun, E. Bleda, C. Trindle, *Life* **2019**, *9*, 34.
[18] J. H. Marks, J. Wang, B.-J. Sun, M. McAnally, A. M. Turner, A. H.-H. Chang, R. I. Kaiser, *ACS Cent. Sci.* **2023**, *9*, 2241.
[19] B. R. Ramachandran, A. M. Halpern, E. D. Glendening, *J. Phys. Chem. A* **1998**, *102*, 3934.
[20] J. Bossa, F. Duvernay, P. Theulé', F. Borget, T. Chiavassa, *Chem. Phys.* **2008**, *354*, 211.
[21] J. A. Noble, P. Theule, F. Duvernay, G. Danger, T. Chiavassa, P. Ghesquiere, T. Mineva, D. Talbi, *Phys. Chem. Chem. Phys.* **2014**, *16*, 23604.
[22] S. Jheeta, S. Ptasinska, B. Sivaraman, N. Mason, *Chem. Phys. Lett.* **2012**, *543*, 208.
[23] J. Demaison, A. G. Császár, I. Kleiner, H. Møllendal, *J. Phys. Chem. A* **2007**, *111*, 2574.
[24] A. D. Becke, *J. Chem. Phys.* **1993**, *98*, 5648.
[25] T. H. Dunning Jr., *J. Chem. Phys.* **1989**, *90*, 1007.
[26] C. Møller, M. S. Plesset, *Phys. Rev.* **1934**, *46*, 618.
[27] K. Raghavachari, G. W. Trucks, J. A. Pople, M. Head-Gordon, *Chem. Phys. Lett.* **1989**, *157*, 479.
[28] R. A. Kendall, T. H. Dunning, R. J. Harrison, *J. Chem. Phys.* **1992**, *96*, 6796.
[29] D. A. Matthews, L. Cheng, M. E. Harding, F. Lipparini, S. Stopkowicz, T.-C. Jagau, P. G. Szalay, J. Gauss, J. F. Stanton, *J. Chem. Phys.* **2020**, *152*, 214108.
[30] J. F. Stanton, J. Gauss, L. Cheng, M. E. Harding, D. A. Matthews, P. G. Szalay, CFOUR, A quantum-chemical program package. **2016**, With contributions from A. Asthana, A.A. Auer, R.J. Bartlett, U. Benedikt, C. Berger, D.E. Bernholdt, S. Blaschke, Y. J. Bomble, S. Burger, O. Christiansen, D. Datta, F. Engel, R. Faber, J. Greiner, M. Heckert, O. Heun, M. Hilgenberg, C. Huber, T.-C. Jagau, D. Jonsson, J. Jusélius, T. Kirsch, M.-P. Kitsaras, K. Klein, G.M. Kopper, W.J. Lauderdale, F. Lipparini, J. Liu, T. Metzroth, L.A. Mück,

D.P. O'Neill, T. Nottoli, J. Oswald, D.R. Price, E. Prochnow, C. Puzzarini, K. Ruud, F. Schiffmann, W. Schwalbach, C. Simmons, S. Stopkowicz, A. Tajti, J. Vázquez, F. Wang, J.D. Watts, C. Zhang, X. Zheng, and the integral packages MOLECULE (J. Almlöf and P.R. Taylor), PROPS (P.R. Taylor), ABACUS (T. Helgaker, H.J.Aa. Jensen, P. Jørgensen, and J. Olsen), and ECP routines by A. V. Mitin and C. van Wüllen. For the current version, see http://www.cfour.de

[31] M. J. Frisch, G. W. Trucks, H. B. Schlegel, G. E. Scuseria, M. A. Robb, J. R. Cheeseman, G. Scalmani, V. Barone, G. A. Petersson, H. Nakatsuji, X. Li, M. Caricato, A. V. Marenich, J. Bloino, B. G. Janesko, R. Gomperts, B. Mennucci, H. P. Hratchian, J. V. Ortiz, A. F. Izmaylov, J. L. Sonnenberg, D. Williams-Young, F. Ding, F. Lipparini, F. Egidi, J. Goings, B. Peng, A. Petrone, T. Henderson, D. Ranasinghe, V. G. Zakrzewski, J. Gao, N. Rega, G. Zheng, W. Liang, M. Hada, M. Ehara, K. Toyota, R. Fukuda, J. Hasegawa, M. Ishida, T. Nakajima, Y. Honda, O. Kitao, H. Nakai, T. Vreven, K. Throssell, J. A. Montgomery Jr., J. E. Peralta, F. Ogliaro, M. J. Bearpark, J. J. Heyd, E. N. Brothers, K. N. Kudin, V. N. Staroverov, T. A. Keith, R. Kobayashi, J. Normand, K. Raghavachari, A. P. Rendell, J. C. Burant, S. S. Iyengar, J. Tomasi, M. Cossi, J. M. Millam, M. Klene, C. Adamo, R. Cammi, J. W. Ochterski, R. L. Martin, K. Morokuma, O. Farkas, J. B. Foresman, D. J. Fox, *Gaussian 16 Revision B.01*, Gaussian Inc., Wallingford CT **2016**.
[32] L. Goerigk, S. Grimme, *J. Chem. Theory Comput.* **2011**, *7*, 291.
[33] S. Grimme, S. Ehrlich, L. Goerigk, *J. Chem. Theory Comput.* **2011**, *32*, 1456.
[34] S. Alessandrini, C. Puzzarini, *J. Phys. Chem. A* **2016**, *120*, 5257.
[35] T. Helgaker, W. Klopper, H. Koch, J. Noga, *J. Chem. Phys.* **1997**, *106*, 9639.
[36] D. E. Woon, T. H. Dunning Jr., *J. Chem. Phys.* **1995**, *103*, 4572.
[37] C. Puzzarini, *J. Phys. Chem. A* **2009**, *113*, 14530.
[38] M. Heckert, M. Kállay, D. P. Tew, W. Klopper, J. Gauss, *J. Chem. Phys.* **2006**, *125*, 44108.
[39] V. Barone, M. Biczysko, J. Bloino, C. Puzzarini, *Phys. Chem. Chem. Phys.* **2013**, *15*, 10094.
[40] D. Feller, *J. Chem. Phys.* **1993**, *98*, 7059.
[41] C. Puzzarini, V. Barone, *Phys. Chem. Chem. Phys.* **2011**, *13*, 7189.
[42] C. Puzzarini, M. Biczysko, V. Barone, *J. Chem. Theory Comput.* **2011**, *7*, 3702.
[43] I. M. Mills, in *Molecular Spectroscopy: Modern Research* (Eds: K. N. Rao, C. W. Matthews), Academic Press, New York **1972**.
[44] W. Gordy, R. L. Cook, *Microwave Molecular Spectra*, Wiley, New York **1984**.
[45] J. Demaison, *Mol. Phys.* **2007**, *105*, 3109.
[46] C. Puzzarini, J. F. Stanton, J. Gauss, *Int. Rev. Phys. Chem.* **2010**, *29*, 273.
[47] J. Gauss, D. Cremer, J. F. Stanton, *J. Phys. Chem. A* **2000**, *104*, 1319.
[48] C. Puzzarini, J. Bloino, N. Tasinato, V. Barone, *Chem. Rev.* **2019**, *119*, 8131.
[49] C. Puzzarini, J. F. Stanton, *Phys. Chem. Chem. Phys.* **2023**, *25*, 1421.
[50] V. Barone, *J. Chem. Phys.* **2005**, *122*, 014108.
[51] J. Vázquez, J. F. Stanton, *Mol. Phys.* **2006**, *104*, 377.
[52] J. V. D. A. Matthews, J. F. Stanton, *Mol. Phys.* **2007**, *105*, 2659.
[53] D. A. Matthews, J. F. Stanton, *Mol. Phys.* **2009**, *107*, 213.
[54] C. Puzzarini, M. Biczysko, V. Barone, *J. Chem. Theory Comput.* **2010**, *6*, 828.
[55] V. Barone, M. Biczysko, J. Bloino, C. Puzzarini, *J. Chem. Phys.* **2014**, *141*, 034107.
[56] P. Pracht, F. Bohle, S. Grimme, *Phys. Chem. Chem. Phys.* **2020**, *22*, 7169.
[57] S. Spicher, S. Grimme, *Angew. Chem. Int. Ed.* **2020**, *59*, 15665.
[58] G. Santra, N. Sylvetsky, J. M. Martin, *J. Phys. Chem. A* **2019**, *123*, 5129.
[59] E. Papajak, D. G. Truhlar, *J. Chem. Theory Comput.* **2011**, *7*, 10.
[60] S. Alessandrini, V. Barone, C. Puzzarini, *J. Chem. Theory Comput.* **2019**, *16*, 988.
[61] J. Lupi, S. Alessandrini, C. Puzzarini, V. Barone, *J. Chem. Theory Comput.* **2021**, *17*, 6974.
[62] T. H. Dunning Jr., K. A. Peterson, A. K. Wilson, *J. Chem. Phys.* **2001**, *114*, 9244.
[63] C. Puzzarini, L. Spada, S. Alessandrini, V. Barone, *J. Phys. Condens. Matter* **2020**, *32*, 343002.
[64] S. Alessandrini, F. Tonolo, C. Puzzarini, *J. Chem. Phys.* **2021**, *154*, 054306.
[65] H. Ye, S. Alessandrini, C. Puzzarini, *Mon. Not. R. Astron. Soc.* **2023**, *525*, 1158.
[66] S. F. Boys, F. Bernardi, *Mol. Phys.* **1970**, *19*, 553.
[67] T. Helgaker, P. Jørgensen, J. Olsen, *Electronic-Structure Theory*, Wiley, Chichester **2000**.
[68] C. Puzzarini, *Phys. Chem. Chem. Phys.* **2004**, *6*, 344.
[69] C. Puzzarini, A. Gambi, *J. Phys. Chem. A* **2004**, *108*, 4138.
[70] J. Demaison, J. Liévin, A. G. Császár, C. Gutle, *J. Phys. Chem. A* **2008**, *112*, 4477.
[71] C. Puzzarini, E. Penocchio, M. Biczysko, V. Barone, *J. Phys. Chem. A* **2014**, *118*, 6648.
[72] A. Halkier, H. Larsen, J. Olsen, P. Jörgensen, J. Gauss, *J. Chem. Phys.* **1999**, *110*, 734.
[73] A. Halkier, W. Klopper, T. Helgaker, P. Jörgensen, *J. Chem. Phys.* **1999**, *111*, 4424.
[74] D. P. Tew, W. Klopper, M. Heckert, J. Gauss, *J. Phys. Chem. A* **2007**, *111*, 11242.
[75] M. A. Cato Jr., D. Majumdar, S. Roszak, J. Leszczynski, *J. Chem. Theory Comput.* **2013**, *9*, 1016.
[76] J. Rezac, P. Hobza, *Chem. Rev.* **2016**, *116*, 5038.
[77] V. Barone, G. Ceselin, M. Fusè, N. Tasinato, *Front. Chem.* **2020**, *8*, 584203.
[78] M. Biczysko, J. Bloino, C. Puzzarini, *WIREs Comput. Mol. Sci.* **2018**, *8*, e1349.
[79] V. Barone, C. Puzzarini, *Ann. Rev. Phys. Chem.* **2023**, *74*, 29.

SUPPORTING INFORMATION

Additional supporting information can be found online in the Supporting Information section at the end of this article.

How to cite this article: C. Puzzarini, S. Alessandrini, *J. Comput. Chem.* **2024**, *45*(29), 2501. https://doi.org/10.1002/jcc.27442